

Attenuation Lengths of Photoelectrons in Fluorocarbon Films

Ramon Colorado, Jr.[†] and T. Randall Lee*

Department of Chemistry, University of Houston, 4800 Calhoun Road, Houston, Texas 77204-5003

Received: May 6, 2003

A series of self-assembled monolayers (SAMs) derived from segmentally perfluorinated alkanethiols, $F(CF_2)_n(CH_2)_{11}SH$, where $n = 4, 6, 8, 10$, on gold was used to measure the attenuation lengths, λ , of photoelectrons possessing kinetic energies between 900 and 1400 eV in fluorocarbon films. The intensities of the photoelectron peaks from the gold substrates decreased exponentially with increasing n , giving attenuation lengths of 40 Å at 1403 eV, 34 Å at 1151 eV, and 25 Å at 940 eV. The attenuation lengths for photoelectrons in the fluorocarbon films were indistinguishable from those in hydrocarbon films measured with SAMs derived from n -alkanethiols on gold.

Introduction

Electron spectroscopies can be used to evaluate the composition and/or structural properties of materials in a quantitative fashion provided that the following two parameters are known: (1) the chemical environment of the material and (2) the attenuation lengths (λ) of the emanating electrons as a function of their kinetic energy (KE).^{1–3} The intensity (I) of Auger electrons or photoelectrons emitted from an element A in a substrate that is covered with a homogeneous overlayer film of thickness τ is described by

$$I_A = I_{A_0} \exp[-\tau/(\lambda \sin \alpha)] \quad (1)$$

where A_0 is the element in a bare substrate and α is the angle between the surface parallel and the analyzer axis (i.e., the takeoff angle).^{1,3} Equation 1 shows that the attenuation length of electrons of given kinetic energies in the overlayer can be determined by measuring the change in the intensities of electrons as a function of a known variation in film thickness. Furthermore, absolute values of λ can vary dramatically with the composition of the attenuating overlayer.^{1,2}

For hydrocarbon films, Bain and Whitesides determined the attenuation lengths of photoelectrons with kinetic energies in the range 900–1400 eV by using X-ray photoelectron spectroscopy (XPS) to analyze self-assembled monolayers (SAMs) on gold derived from the adsorption of n -alkanethiols.⁴ This film/substrate system is ideally suited for determining attenuation lengths because the thickness of the film can be precisely adjusted by varying the chain length of the n -alkanethiols. Later, Laibinis, Bain, and Whitesides extended the range of kinetic energies to 500–1400 eV by studying n -alkanethiolate SAMs on copper and silver substrates.⁵ In more recent studies of n -alkanethiolate SAMs on gold, Lamont and Wilkes used XPS with varied incident photon energies to analyze photoelectrons having even lower kinetic energies (i.e., 140–1100 eV).⁶

Although the aforementioned studies have advanced our understanding of the behavior of electrons in hydrocarbon films, there have been, to our knowledge, no analogous studies

regarding the behavior of electrons in fluorocarbon films.⁷ Much current research targets the use of fluorocarbon materials as thin-film coatings for the purposes of lubrication, thermal resistance, chemical inertness, adhesion, and wetting in a wide range of technological applications.⁸ However, because the attenuation lengths of photoelectrons in fluorocarbons have never been measured directly, characterization of these films using electron spectroscopies has relied thus far on the assumption that fluorocarbons and hydrocarbons attenuate photoelectrons equivalently.^{9–12} The substitution of fluorine atoms for hydrogen atoms in organic compounds has afforded materials with unique chemical and physical properties, whose existence is partly a result of the greater atomic size of fluorine compared to hydrogen.^{8,9} Due to their larger size, fluorine atoms would be expected to scatter photoelectrons to a greater degree than hydrogen atoms; however, the presence of the larger fluorine atoms might also alter the molecular density and physical structure of the organic film to affect the overall attenuation of photoelectrons. In an effort to determine how the structural differences between fluorocarbons and hydrocarbons affect photoelectron attenuation and to lay the groundwork for more detailed analyses of the chemical and structural properties of these materials, we sought to directly measure the attenuation lengths of electrons in fluorocarbon thin films using a system that maintains both molecular density and physical structure constant, while varying the thickness of the fluorocarbon overlayer.

To this end, we synthesized a series of segmentally perfluorinated alkanethiols ($F(CF_2)_n(CH_2)_{11}SH$, where $n = 4, 6, 8, 10$; series 1; denoted FnH11SH), used them to prepare SAMs on gold, and analyzed the resultant SAMs by XPS.¹³ The overlayer films generated from these adsorbates consist of a hydrocarbon region of constant thickness located immediately above the gold surface, followed by a fluorocarbon region in which the thickness increases incrementally with n (Figure 1). Accordingly, the attenuation of electrons from the gold substrates in this series is expected to vary solely as a function of the thickness of the fluorocarbon layer. In the analyses by XPS, we monitored the attenuation of the Au 4f_{7/2}, Au 4d_{5/2}, and Au 4p_{3/2} photoelectrons with kinetic energies in the range 900–1400 eV from the gold substrate through the fluorocarbon films (Figure 2). For comparison, we also monitored the attenuation

* Corresponding author. E-mail: trlee@uh.edu.

[†] Current address: Center for Biological and Environmental Nanotechnology, Department of Chemistry, Rice University, 6100 Main St., Houston, TX 77005.

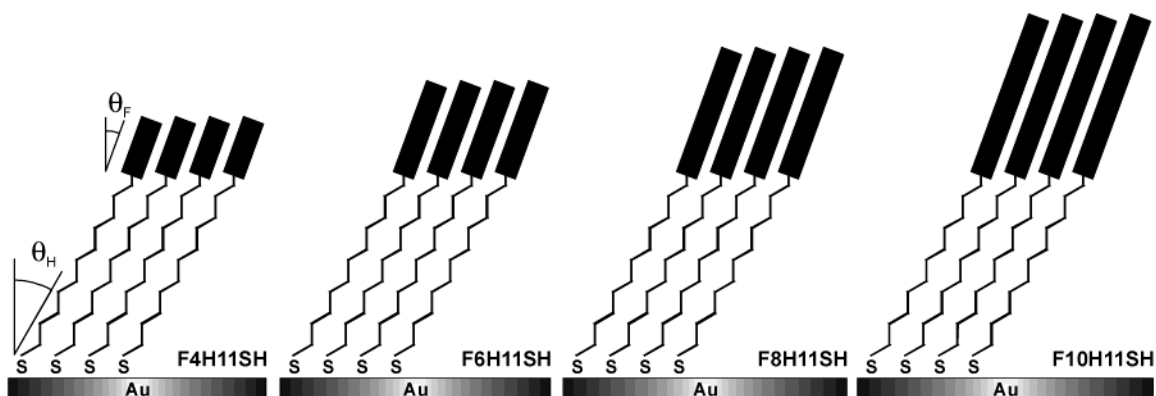


Figure 1. Illustration of SAMs on gold derived from the segmentally fluorinated alkanethiols, FnH11SH (series 1). The hydrocarbon segments are represented by the zigzag lines, and the fluorocarbon segments are represented by the filled rectangles. The average tilt angles of these segments, $\theta_H = 32^\circ$ and $\theta_F = 20^\circ$, are shown.¹⁴

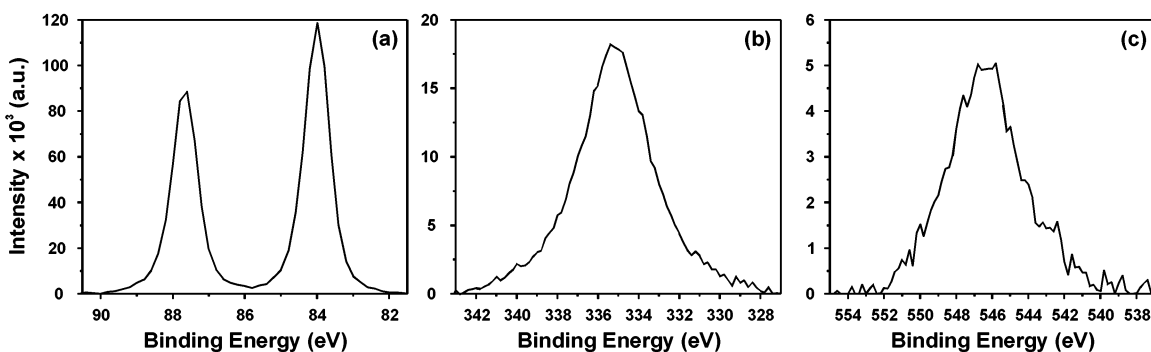


Figure 2. High-resolution X-ray photoelectron spectra of the (a) Au 4f_{7/2}, (b) Au 4d_{5/2}, and (c) Au 4p_{3/2} regions for the SAM on gold derived from F10H11SH. The data illustrate representative signal-to-noise ratios in these studies.

of the photoelectrons through hydrocarbon films using SAMs on gold derived from a series of *n*-alkanethiols (H(CH₂)_mSH, where *m* = 8, 10, 12, 14, 16, 18; series 2; denoted CmSH).

Experimental Section

Materials. Gold shot (99.99%) was purchased from American Precious Metals, and chromium rods (99.9%) were purchased from R. D. Mathis Co. Polished silicon (100) wafers were purchased from North East Silicon Technologies, Inc., and were washed extensively before use. Absolute ethanol was purchased from McCormick Distilling Co. Reagent-grade dichloromethane and toluene were purchased from EM Science. The segmentally perfluorinated alkanethiols used in this study were synthesized using procedures established in our group.^{14,15} After purification, the isolated compounds exhibited spectral data that were consistent with those reported in the literature.^{14–16} The *n*-alkanethiols used in this study were either purchased from Aldrich Chemical Co. or synthesized using common procedures.

Preparation and Characterization of SAMs. Gold substrates were prepared by thermally evaporating an adhesion layer of ca. 100 Å of chromium followed by ca. 2000 Å of gold at a rate of 1 Å/s onto the polished surfaces of the silicon wafers. Deposition pressures were maintained at ca. 8×10^{-6} Torr. The freshly prepared gold-coated wafers were cut into slides (ca. 1 cm × 3 cm) using a diamond-tipped stylus. The slides were washed with absolute ethanol, blown dry with ultrapure nitrogen, and immersed in solutions of the respective thiols (1 mM in ethanol) for no less than 24 h. The solutions were prepared in weighing bottles that were cleaned by soaking in piranha solution (3:1 H₂SO₄/H₂O₂) for 1 h. **Caution:** Piranha solution reacts violently with organic materials and should be handled carefully! The bottles were then rinsed extensively with

deionized water and absolute ethanol. Upon removal from solution, the resultant SAMs were rinsed sequentially with dichloromethane, toluene, and ethanol to remove any physisorbed material. Finally, the films were blown dry with ultrapure nitrogen prior to immediate characterization. Analyses of the films by optical ellipsometry and polarization modulation reflection absorption infrared spectroscopy (PM-IRRAS) were consistent with those previously reported.¹³ Measurements of the wettabilities of the films using contact angle goniometry were consistent with the formation of well ordered films.¹⁷

XPS Analysis of SAMs. A PHI 5700 X-ray photoelectron spectrometer equipped with a 350 W monochromatic Al K α X-ray source ($h\nu = 1486.6$ eV) incident at 90° relative to the axis of a hemispherical energy analyzer was used to obtain spectra of freshly prepared samples. The spectrometer was configured to operate at high resolution with a pass energy of 23.5 eV, a photoelectron takeoff angle (α) of 45° from the surface parallel, and an analyzer spot diameter of 800 μ m. For a given film, spectra were collected at room temperature with a base pressure of 3×10^{-9} Torr for the following photoelectrons: Au 4f_{7/2} (20 eV window; 2 scans over 10 s), Au 4d_{5/2} (20 eV window; 6 scans over 30 s), Au 4p_{3/2} (30 eV window; 9 scans over 45 s), C 1s (25 eV window, 8 scans over 40 s), and F 1s (20 eV window, 6 scans over 30 s). To reduce systematic errors, the films were analyzed in random order. To minimize damage to the films induced by X-rays, total acquisition times for a given spot were limited to less than 3 min.^{6,8} For all SAMs, spectra of the O 1s region (22 eV window, 2 scans over 10 s; collected during the analyses) failed to detect the presence of any oxidized species, and spectra of the S 2p region (20 eV window, 20 scans over 100 s; collected after the analyses) detected only gold-bound sulfur species (BE = 161.9

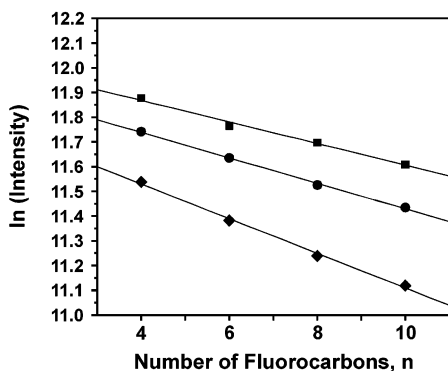


Figure 3. Intensities of the Au 4f_{7/2} (■), Au 4d_{5/2} (●), and Au 4p_{3/2} (◆) photoelectrons as a function of n in SAMs derived from series 1. The data for Au 4p_{3/2} have been raised vertically by 0.8 for clarity.

eV).^{18–21} Multipak V5.0A (Physical Electronics, Inc.) was used to resolve the peak intensities using Shirley background subtraction. For a given SAM, peak intensities were averaged over at least two different spots per slide and at least two slides per sample. All peaks were referenced to the Au 4f_{7/2} peak at a binding energy (BE) of 84.0 eV. As a result, the Au 4d_{5/2}, Au 4p_{3/2}, and F 1s peaks exhibited binding energies of 335.2, 546.5, and 688.6 eV, respectively. The C 1s spectra contained peaks that corresponded to the CH₂, CF₂, and CF₃ regions of the films and exhibited binding energies of 284.6, 291.1, and 293.4 eV, respectively.^{8,22} The resolution of the peaks for the Au 4f_{7/2}, Au 4d_{5/2}, Au 4p_{3/2}, F 1s, and C 1s regions was 0.8, 4.0, 4.9, 1.7, and 1.2 eV, respectively. Linear regression of the data using the least-squares method was performed using Microsoft Excel XP. Errors in the measurements presented in Figure 3 are within the size of the data points.

Results and Discussion

The intensities of the gold photoelectrons in SAMs derived from both series 1 and series 2 are assumed to follow eq 1. The attenuation of these intensities as a function of film thickness can be evaluated by taking logarithms on both sides of eq 1 to give

$$\ln(I_{\text{Au}}) = -\tau/(\lambda \sin \alpha) + \text{constant} \quad (2)$$

For a series of SAMs having constant adsorbate packing density, the film thickness is given by the following function: $\tau = xd$, where x is the number of incremental units per adsorbate, and d is the length per incremental unit.^{4–6} For n -alkanethiolate SAMs on gold (series 2), $x = m$, the number of CH₂ groups per adsorbate, and d , the monolayer thickness per CH₂ group, is calculated by multiplying the chain length (1.27 Å per CH₂ group; derived from X-ray diffraction studies of n -alkanes) by the cosine of the average tilt angle of the alkyl chains from the surface normal (30°; derived from infrared reflection absorption spectroscopy (IRRAS) studies of n -alkanethiolate SAMs on gold) to give a value of $d = 1.27 \cos 30^\circ$, which corresponds to $d = 1.10$ Å.^{4–6} Substitution of these values for τ in eq 2 reveals that a plot of $\ln(I_{\text{Au}})$ versus x should give a straight line with slope equal to $d/(\lambda \sin \alpha)$, which can be manipulated to yield λ .

Accurate determination of λ for fluorocarbon films using SAMs derived from series 1 requires knowledge of the influence of both the hydrocarbon and the fluorocarbon segments on the film thickness. In general, the adsorbate packing density in fluorinated alkanethiolate SAMs on gold varies nonlinearly with the size of the terminal perfluoroalkyl segment.^{12,23,24} SAMs

TABLE 1: Photoelectron Intensity Ratios for SAMs on Gold Derived from Series 1

SAM	C 1s(CH ₂)/Au 4f _{7/2}	C 1s(CF ₂)/Au 4f _{7/2}	F 1s/Au 4f _{7/2}
F4H11SH	0.108 ± 0.007	0.033 ± 0.002	0.54 ± 0.03
F6H11SH	0.101 ± 0.006	0.053 ± 0.004	0.77 ± 0.04
F8H11SH	0.096 ± 0.004	0.081 ± 0.001	1.00 ± 0.02
F10H11SH	0.090 ± 0.007	0.107 ± 0.006	1.24 ± 0.06

derived from series 1, however, all exhibit equivalent 2-D lattice constants of ca. 5.8 Å, as measured by atomic force microscopy (AFM),²⁴ demonstrating that the packing density is constant across this series. In certain previous studies of fluorinated alkanethiolate SAMs on gold,^{12,14,25} we examined the structural properties of films generated from a series of adsorbates possessing perfluorodecyl terminal segments and hydrocarbon segments having variable lengths (i.e., F(CF₂)₁₀(CH₂)_ySH, F10HySH).^{12,14,25} Both IRRAS and near edge X-ray absorption fine structure spectroscopy (NEXAFS) revealed that the tilt angle from the surface normal of the fluorocarbon segments (θ_F) depended on the length of the hydrocarbon segments; specifically, θ_F increased as y increased.^{14,25} The tilt angles of the fluorocarbon and the hydrocarbon segments (θ_H) within SAMs on gold derived from F10H11SH were estimated with NEXAFS to be $\theta_F = 20 \pm 5^\circ$ and $\theta_H = 32 \pm 4^\circ$.¹⁴ Given these data, we can assume with confidence that the tilt angles of the shorter perfluorinated segments in SAMs derived from series 1 (F8, F6, and F4) also equal $20 \pm 5^\circ$, because the length of the hydrocarbon spacer in this series remains constant at eleven methylene units (see Figure 1), and the 2-D lattice spacing of the tail groups remains constant at ca. 5.8 Å.²⁴

To determine whether θ_H remains constant in SAMs derived from series 1, we examined the C/Au intensity ratio of the C 1s(CH₂) and Au 4f_{7/2} photoelectron peaks. Given the constant adsorbate packing density, any changes in θ_H should lead to corresponding variations in the C/Au ratio. Table 1 shows, however, that the C 1s(CH₂)/Au 4f_{7/2} ratios remain roughly constant throughout series 1, suggesting that variations of θ_H with n are negligible. We can therefore assume a constant thickness for the hydrocarbon regions in all of the SAMs derived from series 1 and thus an equivalent attenuation of the gold photoelectrons due to the hydrocarbon region of these SAMs. Consequently, any observed variations in the attenuation of the gold photoelectron intensities for SAMs derived from series 1 can be attributed solely to the variations in the thickness of the fluorocarbon region of these SAMs.

The C 1s(CF₂)/Au 4f_{7/2} and F 1s/Au 4f_{7/2} ratios provided in Table 1 show that increasing n indeed corresponds to a systematic increase in the thickness of the fluorocarbon overlayer. It follows that the attenuation lengths for the gold photoelectrons through fluorocarbon films can be estimated from eq 2 using a plot of $\ln(I_{\text{Au}})$ versus x . In this analysis, $x = n$, the number of CF₂ groups per adsorbate, and d , the thickness of the fluorocarbon layer per CF₂ group, is calculated by multiplying the chain length (1.30 Å per CF₂ group; derived from X-ray diffraction studies of perfluoroalkanes)^{9,14,26,27} by the cosine of the average tilt angle of the fluorocarbon chains from the surface normal (20°; vide supra) to give a value of $d = 1.30 \cos 20^\circ$, which corresponds to $d = 1.22$ Å.

Figure 3 plots the natural log of the intensities of the Au 4f_{7/2}, Au 4d_{5/2}, and Au 4p_{3/2} photoelectrons versus n (for SAMs derived from Series 1). Table 2 shows the slopes and the derived attenuation lengths for SAMs derived from series 1.²⁸ The good linear fits of the data confirm the appropriateness of eq 1 in describing the behavior of photoelectrons in this series. The attenuation lengths for this series exhibit the expected decrease

TABLE 2: Attenuation Lengths Calculated from Gold Photoelectron Intensities in SAMs on Gold Derived from Series 1

photoelectron	KE (eV)	slope	λ (Å)
Au 4f _{7/2}	1403	-0.044	40 ± 3
Au 4d _{5/2}	1151	-0.051	34 ± 1
Au 4p _{3/2}	940	-0.070	25 ± 1

with decreasing kinetic energy of the photoelectrons.⁴⁻⁶ In addition, the attenuation lengths measured for the hydrocarbon films of series 2 [$\lambda(\text{Au } 4f_{7/2}) = 40 \pm 3 \text{ \AA}$, $\lambda(\text{Au } 4d_{5/2}) = 32 \pm 2 \text{ \AA}$, $\lambda(\text{Au } 4p_{3/2}) = 26 \pm 2 \text{ \AA}$] are entirely consistent with those reported previously (see Figure S1 and Table S1 in the Supporting Information).^{4-6,29} Comparison of these data with those in Table 2 indicates that the attenuation lengths of photoelectrons in SAMs derived from series 1 are indistinguishable from those in SAMs derived from series 2, which leads to the conclusion that electrons with kinetic energies between 900 and 1400 eV are attenuated equally by close-packed and well-ordered fluorocarbons and hydrocarbons.

Suzuki et al. have shown that the attenuation lengths of photoelectrons in organic thin films are dependent on the following three parameters: (1) the elemental composition, which determines the different electron scattering cross-sections present in the films, (2) the atomic densities, because a denser collection of atoms increases attenuation, and (3) the film structure (i.e., molecular orientation and packing density within the film), which dictates the optimum atomic density and overlayer thickness.³⁰ The films derived from series 1 all possess attenuating overlayers consisting of only carbon and fluorine. Furthermore, the densities of these atoms in the overlayer are determined by the packing density and molecular tilt of the segmentally perfluorinated alkanethiol adsorbates, which we have shown to remain constant within films of series 1. Therefore, the only parameter that changes within series 1 as the number of CF₂ groups per adsorbate is increased is the overlayer thickness. The identical argument can be made for films of series 2, with the exception that the elemental composition of the overlayer consists of only carbon and hydrogen.

Comparison of the parameters pertaining to films of series 1 with those of series 2 provides insight into the observed results. At the atomic level, the replacement of hydrogen with fluorine in the overlayer is expected to increase the photoelectron attenuation because fluorine possesses a larger electron scattering cross-section.²² However, because the data indicate that photoelectrons are not significantly attenuated more by fluorocarbon films, a change in the structure of films of series 1 that leads to a lower atomic density of fluorine (and hence lower electron scattering) must occur.

The substitution of fluorine atoms for hydrogen atoms in a trans-extended alkyl chain is expected to increase the molecular volume due to the larger size of fluorine atoms.⁹ The presence of the fluorine atoms, however, also produces unfavorable 1,3-diaxial repulsions that are relieved by the carbon chain adjusting its conformation from trans-extended to helical.²⁷ These effects give rise to the larger van der Waals (vdW) diameter of 5.6 Å for perfluoroalkyl segments compared to that of 4.2 Å for *n*-alkyl segments.^{9,14,26,27} The larger molecular volume of perfluoroalkyl segments is responsible for the decreased packing density of segmentally perfluorinated alkanethiols self-assembled on gold (lattice spacing = 5.8 Å) compared with that of *n*-alkanethiols self-assembled on gold (lattice spacing = 5.0 Å).^{12,23,24}

The structural differences between fluorocarbons and hydrocarbons can be used to rationalize the observed attenuation

lengths. It seems that any increased attenuation arising from the replacement of hydrogen atoms with larger fluorine atoms is offset by the fact that the resulting fluorocarbon segments must pack less densely (i.e., fewer chains per unit area) than the original hydrocarbon segments. Apparently, electrons interact with a quantity of matter in the relatively loosely packed fluorocarbon films that is equivalent to that in the more densely packed hydrocarbon films. In other words, the less densely packed fluorocarbon segments effectively scatter the photoelectrons to the same degree as the more densely packed hydrocarbon segments.

Conclusions

The attenuation lengths of photoelectrons with kinetic energies between 900 and 1400 eV in fluorocarbon films were measured with a series of segmentally fluorinated alkanethiolate SAMs on gold and were compared to those obtained for hydrocarbon films measured with a series of *n*-alkanethiolate SAMs on gold. The attenuation lengths of photoelectrons in the fluorocarbon films decreased with decreasing kinetic energy of the photoelectrons and were found to be indistinguishable from those in hydrocarbon films. The similar attenuation in the fluorocarbon films was attributed to the lower packing densities of segmentally fluorinated moieties compared to those of hydrocarbon moieties, which can plausibly counteract the increased attenuation that might be anticipated by substituting relatively small hydrogen atoms with larger fluorine atoms. The trends in electron attenuation presented here should not be limited to SAMs on gold, but should also be valid in other systems in which semicrystalline fluorocarbon films are composed of helical perfluoroalkyl segments.

Acknowledgment. The National Science Foundation (DMR-9700662), the Texas Advanced Research Program (003652-0307-2001), and the Robert A. Welch Foundation (E-1320) provided generous support for this research. This work made use of MRSEC shared experimental facilities supported by the National Science Foundation (DMR-9632667). R.C. kindly thanks the National Research Council-Ford Foundation and the University of Houston Center for Mexican-American Studies for predoctoral fellowships. We also thank Mr. H. Justin Moore and Mr. Joon-Seo Park for assisting with sample preparation.

Supporting Information Available: Figure of intensities as a function of the number of carbons and table of attenuation lengths for hydrocarbon SAMs on gold (series 2). This material is available free of charge via the Internet at <http://pubs.acs.org>.

References and Notes

- Briggs, D.; Seah, M. P. *Practical Surface Analysis*, 2nd ed.; Wiley: Chichester, 1990; Chapters 1, 3-5, 9.
- Ratner, B. D.; Castner, D. G. In *Surface Analysis-The Principle Techniques*; Vickerman, J. C., Ed.; Wiley: Chichester, U.K., 1997; p 43.
- The probability of an electron with a given kinetic energy escaping without significant energy loss due to inelastic scattering drops to 1/e of its original value at a distance normal to the surface that is defined as the escape depth. The terms attenuation length and escape depth are often used interchangeably. The attenuation length is only identical to the inelastic mean free path, the average distance that an electron with a given kinetic energy travels between successive inelastic collisions, in the absence of elastic scattering.^{1,2}
- Bain, C. D.; Whitesides, G. M. *J. Phys. Chem.* **1989**, *93*, 1670.
- Laibinis, P. E.; Bain, C. D.; Whitesides, G. M. *J. Phys. Chem.* **1991**, *95*, 7017.
- Lamont, C. L. A.; Wilkes, J. *Langmuir* **1999**, *15*, 2037.

- (7) An evaluation of the attenuation length of C 1s photoelectrons from a fluorocarbon lubricant layer on a carbon-coated magnetic disk has been reported: Nishimori, K.; Tanaka, K.; Sato, K. *J. Vac. Sci. Technol.* **1990**, *A8* (4), 3300.
- (8) Castner, D. G.; Grainger, D. W. *Fluorinated Surfaces, Coatings, and Films*; ACS Symposium Series 787; American Chemical Society: Washington, DC, 2001.
- (9) Grainger, D. W.; Stewart, C. W. In *Fluorinated Surfaces, Coatings, and Films*; Castner, D. G., Grainger, D. W., Eds.; ACS Symposium Series 787; American Chemical Society: Washington, DC, 2001; p 1.
- (10) Tsao, M.-W.; Hofmann, C. L.; Rabolt, J. F.; Johnson, H. E.; Castner, D. G.; Erdelen, C.; Ringsdorf, H. *Langmuir* **1997**, *13*, 4317.
- (11) Tsao, M.-W.; Rabolt, J. F.; Schonherr, H.; Castner, D. G. *Langmuir* **2000**, *16*, 1734.
- (12) Tamada, K.; Ishida, T.; Knoll, W.; Fukushima, H.; Colorado, R., Jr.; Graupe, M.; Shmakova, O. E.; Lee, T. R. *Langmuir* **2001**, *17*, 1913.
- (13) Colorado, R., Jr.; Graupe, M.; Shmakova, O. E.; Villazana, R. J.; Lee, T. R. In *Interfacial Properties on the Submicron Scale*; Frommer, J. E., Overney, R., Eds.; ACS Symposium Series 781; American Chemical Society: Washington, DC, 2001; p 276.
- (14) Frey, S.; Heister, K.; Zharnikov, M.; Grunze, M.; Tamada, K.; Colorado, R., Jr.; Graupe, M.; Shmakova, O. E.; Lee, T. R. *Isr. J. Chem.* **2000**, *40*, 81.
- (15) Graupe, M.; Takenaga, M.; Koini, T.; Colorado, R., Jr.; Lee, T. R. *J. Am. Chem. Soc.* **1999**, *121*, 3222.
- (16) Naud, C.; Calas, P.; Blancou, H.; Commeyras, A. *J. Fluorine Chem.* **2000**, *104*, 173.
- (17) Colorado, R., Jr.; Lee, T. R. *Langmuir* **2003**, *19*, 3288.
- (18) Laibinis, P. E.; Whitesides, G. M.; Allara, D. L.; Tao, Y.-T.; Parikh, A. N.; Nuzzo, R. G. *J. Am. Chem. Soc.* **1991**, *113*, 7152.
- (19) Castner, D. G.; Hinds, K.; Grainger, D. W. *Langmuir* **1996**, *12*, 5083.
- (20) Schoenfish, M. H.; Pemberton, J. E. *J. Am. Chem. Soc.* **1998**, *120*, 4502.
- (21) Hutt, D. A.; Leggett, G. J. *J. Chem. Phys.* **1996**, *100*, 6657.
- (22) Moulder, J. F.; Stickle, W. F.; Sobol, P. E.; Bomben, K. D. *Handbook of X-ray Photoelectron Spectroscopy*; Physical Electronics: Eden Prairie, MN, 1995.
- (23) Schonherr, H.; Vansco, G. J. In *Fluorinated Surfaces, Coatings, and Films*; Castner, D. G., Grainger, D. W., Eds.; ACS Symposium Series 787; American Chemical Society: Washington, DC, 2001; p 15.
- (24) Yam, C. M.; Colorado, R., Jr.; Perry, S. S.; Lee, T. R., manuscript in preparation.
- (25) Fukushima, H.; Seki, S.; Nishikawa, T.; Takiguchi, H.; Tamada, K.; Abe, K.; Colorado, R., Jr.; Graupe, M.; Shmakova, O. E.; Lee, T. R. *J. Phys. Chem. B* **2000**, *104*, 7417.
- (26) Bunn, C. W.; Howells, E. R. *Nature* **1954**, *174*, 549.
- (27) Dixon, D. A.; van-Catledge, F. A. *Int. J. Supercomput. Appl.* **1988**, *2*, 62.
- (28) The errors in λ were determined by propagating the standard error of the slopes derived from least squares regression with 95% confidence intervals.
- (29) The values of λ measured in this study are within the error of the values reported in ref 4.
- (30) Suzuki, N.; Imura, K.; Satoh, S.; Saito, Y.; Kato, T.; Tanaka, A. *Surf. Interface Anal.* **1997**, *25*, 650.